Progressive Multi-Source Domain Adaptation for Personalized Facial Expression Recognition

Muhammad Osama Zeeshan ⬡, *Student Member, IEEE,*, Marco Pedersoli ⬡, *Member, IEEE,* Alessandro Lameiras Koerich ⬡, *Member, IEEE,* and Eric Granger ⬡ , *Member, IEEE*

Abstract—**Personalized facial expression recognition (FER) involves adapting a machine learning model using samples from labeled sources and unlabeled target domains. Given the challenges of recognizing subtle expressions with considerable interpersonal variability, state-of-the-art unsupervised domain adaptation (UDA) methods focus on the multi-source UDA (MSDA) setting, where each domain corresponds to a specific subject, and improve model accuracy and robustness. However, when adapting to a specific target, the diverse nature of multiple source domains translates to a large shift between source and target data. State-of-the-art MSDA methods for FER address this domain shift by considering all the sources to adapt to the target representations. Nevertheless, adapting to a target subject presents significant challenges due to large distributional differences between source and target domains, often resulting in negative transfer. In addition, integrating all sources simultaneously increases computational costs and causes misalignment with the target. To address these issues, we propose a progressive MSDA approach that gradually introduces information from subjects (source domains) based on their similarity to the target subject. This will ensure that only the most relevant sources from the target are selected, which helps avoid the negative transfer caused by dissimilar sources. During adaptation, the source domains are introduced in a curriculum manner. We first exploit the closest sources to reduce the distribution shift with the target and then move towards the furthest while only considering the most relevant sources based on the predetermined threshold. Furthermore, to mitigate catastrophic forgetting caused by the incremental introduction of source subjects, we implemented a density-based memory mechanism that preserves the most relevant historical source samples for adaptation. Our extensive experiments [1] show the effectiveness of our proposed method on challenging pain FER datasets: Biovid and UNBC-McMaster. Further, performance is evaluated on a cross-dataset setting *(UNBC-McMaster → BioVid)*, showing the importance of gradually adapting to source subjects.**

Index Terms—**Unsupervised Domain Adaptation, Multi-Source Domain Adaptation, Gradual Domain Adaptation, Facial Expression Recognition, and Pain Estimation.**

I. INTRODUCTION

IN recent years, there has been a growing demand for deep learning (DL) models that can perform well on FER across various industrial sectors such as in detecting suspicious or criminal behavior, automated emotion recognition, or the estimation of pain in health care [1]–[4]. Addressing the significant variability of facial expressions between individuals due to cultural and ethnic differences or varying capture conditions is a challenging problem because of the subtle expression in real-world applications that leads to a substantial disparity between the data used to train and test DL models [5]. Therefore, adapting a deep FER model to a specific individual (i.e., personalization) is important to maintain a high level of performance.

Personalized FER has been extensively studied in the literature, primarily through supervised learning approaches and fine-tuning techniques [6]–[8] to capture individual-specific nuances. These approaches mostly rely on fully or weakly labeled data to adapt and create a personalized model for each subject. Fine-tuning a model using fully labeled data requires a costly annotation of samples and this annotation may be ambiguous due to variability among the annotators [9], [10]. Unsupervised domain adaptation (UDA) [11], [12] is a promising alternative for leveraging unlabeled data in FER. Nevertheless, SOTA UDA techniques treat datasets as domains containing samples from mixed subjects across source and target domains, which limits the model's ability to perform fine-grained adaptation [13]–[15]. Defining each subject as a domain can address this issue yet blending source data to perform UDA restricts its capacity to handle variations and diversity within the target domain. To address this challenge, multi-source (unsupervised) domain adaptation (MSDA) [16]–[18] has gained significant popularity as it incorporates information from multiple source domains to enhance model resilience to different target variations. In [18], the authors introduced a subject-based domain adaptation method, where each domain consists of a distinct subject, thus multiple sources and a single target subject. The target domain consists of samples belonging to a single person, where the data are captured in a stationary environment and incorporate less effective diversity. This approach differs from the traditional MSDA methods that adapt to a target domain of mixed individuals. The subject-based method focused on adapting to a single individual enables more precise and targeted adaptation strategies to create a personalized FER model.

MSDA methods address the challenge of transferring knowledge across diverse domains (datasets) by aligning multiple source domains with a target domain representation. By leveraging data from multiple sources, MSDA aims to enhance model robustness and generalization by minimizing domain shift [19], [20] and create a shared feature space where source and target distributions are closely matched. While effective in some cases, this approach forces all sources to align with the target data, often overlooking individual domain variability. In contrast, the subject-based domain adaptation

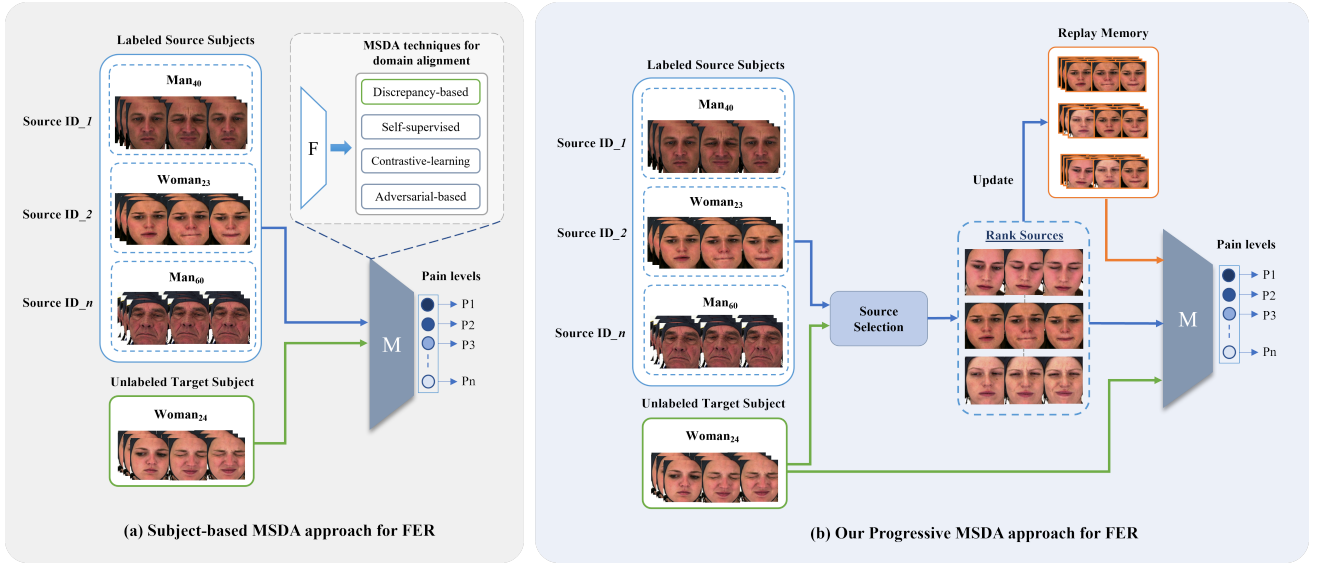[1] https://github.com/osamazeeshan/P-MSDA

Fig. 1: Comparison between the subject-based MSDA approach with our proposed progressive MSDA method. In MSDA, the alignment of domains is a crucial step that can be accomplished through *Discrepancy-based, Self-supervised, Contrastive-learning, or Adversarial-based* approaches. (a) In subject-based MSDA, the model takes advantage of all the source domains during the target adaptation process and performs alignment using the discrepancy-based approach. (b) Our progressive MSDA method consists of two steps. First, we rank and gradually adapt source domains (subjects) based on their similarity to the target domain, optimizing the transfer process through sequential adaptation. Second, to address catastrophic forgetting, we construct a replay memory (domain) that retains key samples from previously adapted source domains, which are re-accessed after each source-target adaptation to maintain knowledge consistency. The discrepancy-based approach is applied to align the source and target domains.

method in [18] struggles with target adaptability under such alignment, as the inherent differences among source subjects can deviate significantly from the target domain. Although the adaptation to all the source subjects is beneficial for learning a better representation of diverse subjects, adapting to a single target subject does not always require incorporating every source subject. This is due to the subject's negative transfer [21], [22] caused by the large difference in distributions of source and target domains. For instance, if the target domain corresponds to a *young caucasian woman* and the source domains consist of a diverse group of individuals from varying personal characteristics such as age, ethnicity, and gender (illustrated in the Fig. 1(a)). Integrating all the source domains will generate a large domain shift between source and target, causing a model to deviate, and creating difficulties in the adaptation process. Furthermore, it would not be feasible in real-world applications due to high computing and memory consumption.

To address the challenges of developing a subject-based MSDA method for FER, we gradually introduce only the most relevant source domains (subjects) during the adaptation process. We introduce a method that integrates curriculum learning (CL) [23] and self-paced learning (SPL) [24], leveraging prior knowledge from CL to prioritize easier source subjects during target domain adaptation. Simultaneously, SPL is employed to dynamically adapt the learning process, allowing the model to recalibrate and select relevant sources as training progresses. To effectively capture contextual information from each source subject while avoiding domain corruption, we

adopt a progressive approach by adapting to one source at a time gradually. Drawing inspiration from domain-incremental learning (DIL) replay techniques [25], [26], where new conditions are incrementally introduced to the target domain while preserving previously learned information. In this work, we propose a replay-based mechanism that dynamically selects and stores the most transferable samples from the visited source domains. This ensures efficient adaptation to the target subject prevents catastrophic forgetting, and reduces computational overhead.

In this paper, we present a new paradigm of MSDA in facial expression recognition that *progressively* adapts to an unlabeled target subject by exploiting the representation of the most relevant source subjects. We hypothesize that domain-level adaptation may be suboptimal in personalized FER, as the distribution of each facial expression is highly unique for each subject. To consider the most relevant sources for the unlabeled target subject, we proposed a progressive multi-source domain adaptation (P-MSDA) leveraging the closest sources for gradual adaptation, allowing a model to learn from individual source representation. Motivated by the concept of "start small" from curriculum learning (CL) [23], we first exploit the source subjects that are closer to the target *(in the feature space)* and gradually introduce new subjects, while taking advantage of SPL to recalibrate and select the most pertinent sources. We compute the similarity matrix of target and source subjects while applying a predetermined threshold. This will ensure focusing only on the most relevant source subjects, as illustrated in Fig. 1(b). To train such a model,

a naive approach begins with the easiest source subject and gradually moves towards the hardest subjects while storing all the previously seen subjects. Another option is to train a model by ignoring the previously learned subjects and only training with the newly added source subject. The former approach requires significant computation power and memory consumption, while the latter setting will lean towards the problem of catastrophic forgetting [27], [28]. To avoid using every visited subject and eliminate the problem of forgetting, we follow the DIL replay-based [29] strategy, where we create a replay dictionary that preserves a small set of previously adapted samples based on the closest source points from the target clusters and only incorporate those with the newly added subject. We keep updating the replay dictionary as the training progresses. Our method aims to strike a balance between leveraging diverse source information and maintaining focus on the target domain's specific characteristics.

The main contributions of this paper are summarized as follows. **(1)** A novel progressive learning framework for MSDA personalized FER that exploits the closest source subjects for target adaptation. Additionally, we present an effective training strategy based on DIL that starts with the closest source and gradually introduces a new subject while limiting the number of source subjects to the *top-N* pertinent sources. This approach minimizes the risk of data corruption from mixed source domains and reduces computational complexity. **(2)** Inspired by the incremental learning replay technique, we present a density-based sample selection mechanism that retains the most relevant samples from previously visited source subjects, avoiding catastrophic forgetting. **(3)** The performance of the proposed method is extensively evaluated on diverse groups of multiple source and target subjects on challenging BioVid and UNBC-McMaster pain estimation datasets. We also show the efficacy of our method by evaluating cross-dataset, specifically UNBC-McMaster (source) to BioVid (target). Further, we present a comprehensive analysis of the selection of previous samples for better target adaptation.

II. RELATED WORKS

A. Personalized Facial Expression Recognition

Personalization in facial expression recognition (FER) focuses on adapting models for specific individuals by considering variations in facial features, cultural nuances, and subjective labeling. In recent years, supervised personalization techniques [6], [7] have gained significant attention, as they aim to enhance model performance using labeled data, which leads to improved accuracy. Despite the progress made, these methods depend on fine-tuning a model using subject-specific labels, which are often unavailable in real-world applications. Another challenge arises from users with extreme facial variations, which can lead to issues with identity bias and temporal dynamics, particularly when dealing with unseen subjects. To tackle these issues, domain adaptation (DA) techniques [13], [15] have been explored. These methods align the feature distributions of labeled (seen) data with subject-specific (unseen) data that is not explicitly labeled.

B. Domain Adaptation

Domain adaptation (DA) methods typically leverage labeled data from a source domain and unlabeled data from a target domain. The DA methods can be categorized into three main types: discrepancy-based, reconstruction-based, and adversarial-based. Discrepancy-based methods [13], [15] aim to minimize domain shift by reducing discriminative features between domains. Reconstruction-based approaches [30], [31] focus on encoding representations of both source and target domains, often utilizing techniques such as deep reconstruction classification models and transfer learning-based auto-encoders. Adversarial-based approaches [32]–[34], employ adversarial techniques to adapt domain representations, such as adversarial graph representation adaptation and augmentation techniques with AC-GAN. Each category offers unique strategies to address the challenge of domain adaptation, contributing to the advancement of visual deep learning models in diverse operational contexts. Although DA-based approaches have provided a robust framework for adapting to an operational target domain. However, the reliance on a single source domain for target adaptation limits the models' exposure to diverse data distributions. This constraint often limits its ability to have an effective target adaptation. To address this limitation, our previous work on subject-based MSDA [18] introduced a novel technique to incorporate multiple source domains (subjects) that demonstrated significant performance improvements and exhibited diversity in source domains.

C. Multi-Source Domain Adaptation

Multi-source domain adaptation (MSDA) enhances target model accuracy and robustness by leveraging multiple labeled source datasets, improving the generalization in the target domain. MSDA methods have been widely adopted in many image classification tasks [16], [19], [35], [36], these techniques can be further classified to mitigate domain shift challenges, adversarial [16], [36], self-supervised [37], [38], and discrepancy-based approaches [19]. Although we have good performance on standard benchmark datasets [35], there is still a gap in how to utilize these techniques when increasing the number of source domains in the recognition of facial expressions. Recently, Zeeshan et al. [18] proposed an MSDA method for subject-based FER, which provides a framework to tackle many source domains, i.e., up to 77, while successfully adapting to the target domain. Nevertheless, this method adapts to the target domain by leveraging multiple source subjects. While the method suggests selecting only the top-k sources, it still relies on aggregating all chosen source domains and performing joint training with the target subject. This strategy, although effective, may introduce potential noise from less relevant source domains. In contrast, our proposed strategy ranked the source domains (subjects) based on their similarity of data distribution with the target domain. Subsequently, it gradually incorporates additional subjects while continuously monitoring and optimizing performance on the target subject. This incremental integration will potentially mitigate the impact of less relevant source domains.

D. Gradual Domain Adaptation

Our work is also closely related to gradual domain adaptation (GDA). In GDA, including intermediate domains helps reduce the significant domain shift between source and target. The source domain adapts to these intermediate domains, gradually bridging the gap between the target domain. Several methods are introduced that help in gradual adaptation, such as using self-training [39]–[41] where intermediate domains were defined, in the absence of intermediate domains [42]. Our approach, inspired by GDA, directly uses the source domains that are closer to the target in the feature space and uses them for the target adaptation instead of going from source to target with the help of intermediate domains. Nevertheless, based on the model selection criteria, we only incorporate source domains that benefit the target.

E. Incremental Learning

Incremental learning involves sequentially acquiring knowledge from a series of datasets without retaining access to previously learned data. It has garnered significant attention in recent years. This framework can be divided into three primary scenarios [43]: task-incremental learning [44], class-incremental learning [45], and domain-incremental learning [25]. In this paper, we focused on domain-IL for exploiting the source subjects in target adaptation. Domain incremental learning (DIL) refers to sequentially adapting to new domains without forgetting the prior information. Typically, DIL-based techniques were applied to target domains such as image classification [25], autonomous driving to detect objects [46], and semantic segmentation [47], where it is necessary to preserve the knowledge gained in the previous domain. To eliminate catastrophic forgetting, these techniques were categorized into three groups. Parameter isolation [48] stores a network or useful model parameters from previous data that is utilized with a new domain. The regularization-based strategy updates the loss by introducing regularization terms using techniques such as knowledge distillation [49], [50], which gives weight to pertinent features. Replay-based approaches [29] store some previous data by either storing them directly [49] or generating them using GAN-based techniques [28], [51]. In addition, incremental learning approaches are also applied in domain adaptation when multiple target domains exist. Wei et al. [52] proposed a distillation function to acquire previously learned knowledge. Similarly, Kiran et al. [53] adapt to multiple target domains incrementally by training a domain transfer module that generates the pseudo-images of previous targets. However, DIL-based domain adaptation methods focus on increasing target domains while retaining knowledge of the past domains, and typically overlook the domain shift problem. In contrast, the proposed technique adapts to a single unlabeled target and focuses on incrementally introducing the source domains while preserving only the most relevant samples by mitigating discrepancies between the domains to improve target adaptability.

F. Self-paced Curriculum Learning

Curriculum learning (CL) [23] and self-paced learning (SPL) [24] have been widely adopted in many machine learning and computer vision tasks. Both learning paradigms follow a structured approach, starting with simpler tasks and progressively transitioning to more complex ones. Specifically, CL leverages prior knowledge from multiple source domains to guide the learning process while SPL dynamically adjusts to the model learning pace during training. Choi et al. [54] proposed a CL-based technique for UDA. It applies CL to introduce the target pseudo-labels based on the density clustering method; it picks the subset with high density first and moves towards the lower-density samples later. Wang et al. [55] introduced an SPL-based approach that considers easy samples from the target domain based on the agreement on the predictions from the source classifiers. Initially, these classifiers are trained on the individual source domains, and then a single classifier, including all the domains, is trained. If both classifiers agree, those samples will be included first in the training process. Jiang et al. [56], propose self-paced curriculum learning (SPCL), a unified framework that integrates prior knowledge with adaptive learning progress. Formulated as an optimization problem, SPCL balances the strengths of both approaches by incorporating fixed prior knowledge and dynamically refining the curriculum throughout training. Yang et al. [57] proposed a CL-based MSDA method that relies on domain discriminator loss for the selection. The samples with a similar distribution as the target are more challenging for the discriminator to separate and are selected first. However, these approaches do not consider how the source samples were introduced; instead, they focus on presenting the most confident target samples in the training protocol. Furthermore, Yang et al. [57] technique utilizes all the samples in the source domain, which is relatively ineffective in subject-based FER scenarios as they do not consider the domain negative impact that drifts the model for adapting to a particular target subject. Hence, novel approaches are required to handle this challenge effectively.

III. PROPOSED APPROACH

Fig. 2 provides an overview of the P-MSDA framework, which dynamically generates a curriculum of source subjects, ranging from the easiest to the hardest, gradually introduced to a given target domain (Sec. III-B), followed up by the creation of a dynamic replay dictionary (domain) of the most representative source distributions that helps in preventing catastrophic forgetting during the adaptation process (Sec. III-C).

A. Preliminaries

In MSDA, given a set of labeled source domains $\mathcal{S} = \{\mathbf{S}_1, \mathbf{S}_2, \ldots, \mathbf{S}_a, \ldots, \mathbf{S}_D\}$ and a single unlabeled target domain $\mathbf{T}$, where $a = \{1, 2, \ldots, D\}$ is the number of source domains. To preserve relevant samples from previous source domains, we define a replay domain $\mathbf{R}$. We define a source domain as $\mathbf{S}_a = \{(\mathbf{x}_i^s, y_i^s)\}_{i=1}^{N^s}$, where N^s represents the number of samples within each source domain a. Assuming that $\mathbf{x}_i^s$ represents an input embedding of a source domain sample i produced by an
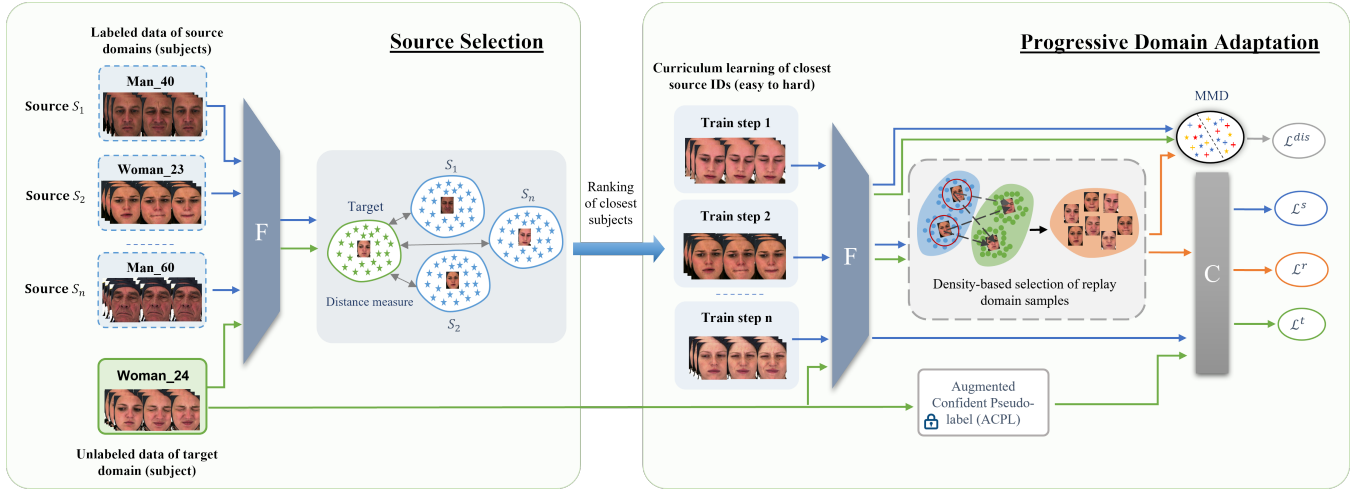
Fig. 2: Overview of our proposed progressive MSDA method for the adaptation to the target subject. **Source Selection Phase:** We estimate the similarity matrix between every source and target embedding, followed by ranking the sources from most to least similar subjects. **Progressive Domain Adaptation Phase:** Ranked sources are progressively incorporated through iterative training steps (*Train Step-1*, *Train Step-2*, ..., *Train Step-n*). At each step, a new source subject is introduced and aligned with the target by calculating discrepancy and supervised losses. The Augmented Confident Pseudo-label (ACPL) technique from [18] generates reliable pseudo-labels for the target. Finally, we create a replay dictionary using a density-based selection to preserve previously visited relevant source samples

encoder F, the labeled source domain input space is defined as $\mathbf{x}_i^s$, and their respective labels as y_i^s. We define a single unlabeled target domain as $\mathbf{T} = \{\mathbf{x}_i^t\}_{i=1}^{N^t}$, where N^t denotes the number samples within the target domain. A replay domain is defined as $\mathbf{R} = \{(\mathbf{x}_i^r, y_i^r)\}_{i=1}^{N^r}$, where N^r represents the number of relevant source domains from $\mathcal{S}$, which keeps on updating after adapting the model Θ to the target domain $\mathbf{T}$. The model Θ integrates the representation learning module F with the classifier C. The objective is to leverage the information of source domains by gradually introducing domains from $\mathcal{S}$ to improve the performance of a model Θ on the target domain $\mathbf{T}$. Therefore, at each training step, the model Θ aims to learn from a new source domain from $\mathcal{S}$ and $\mathbf{R}$, which retain the most representative information from the previous source domains.

B. Source Selection

Before progressive adaptation of the model Θ to the target domain, we aim to select the most suitable domains from a multi-source domain $\mathcal{S}$ to align them with the target domain $\mathbf{T}$, based on a curriculum-based approach. Initially, we prioritize the source domains with high transferability to align them with the target domain. This will help select source domains with feature distributions similar to the target domain. After aligning the feature distributions of these source domains, a source selection[1] will prioritize the next round of source domains for alignment. As adaptation (training) continues, the model Θ gradually learn to focus on various aspects of the feature distribution to improve transferability. Our approach involves learning a curriculum to prioritize different source domains. We hypothesize that source domains closest to the target domain in the feature space are the ones that are easier

for the model to adapt to. We compute the cosine similarity between every source domain and the target domain in a mini-batch [58], where the domains are represented by their feature embeddings as:

$$h(\mathbf{x}^s, \mathbf{x}^t) = \frac{\mathbf{x}^s \cdot \mathbf{x}^t}{\|\mathbf{x}^s\|_2 \cdot \|\mathbf{x}^t\|_2} \quad (1)$$

where $\|.\|_2$ is the ℓ^2-norm of the feature embeddings.

Assuming a mini-batch of size B, where $X^s = \{\mathbf{x}_1^s, \mathbf{x}_2^s, \ldots, \mathbf{x}_B^s\}$ and $X^t = \{\mathbf{x}_1^t, \mathbf{x}_2^t, \ldots, \mathbf{x}_B^t\}$ represent feature embeddings from the source and target domains in the mini-batch, and N^b is the total number of batches, a pair-wise similarity matrix is calculated as:

$$\mathbf{M}^c(\mathcal{S}, \mathbf{T}) = \frac{1}{N^b} \sum_{i=1}^{N^b} h(X_i^s, X_i^t) \quad (2)$$

To estimate the similarity matrix for all the source and target domain pairs, we define:

$$P = [\mathbf{M}^c(\mathbf{S}_1, \mathbf{T}), \ldots, \mathbf{M}^c(\mathbf{S}_D, \mathbf{T})] \quad (3)$$

where $\mathbf{M}^c(.)$ is the cosine similarity between every feature embedding in $\mathcal{S}$ and $\mathbf{T}$, D represents the total number of sources domains, and P is a dictionary (list) that stores all pair-wise distances indexed by the respective source domain information. To determine the stopping criteria for including source domains in the adaptation process, we apply a normalization procedure on similarity measures in P to scale them to the range $[0, 1]$ and we obtain $\widetilde{P}$, which is the scaled version of P. Subsequently, we apply a predetermined threshold γ to $\widetilde{P}$ to limit the number of source domains. We formulate the process of selecting source domains as:

$$\widetilde{\mathcal{S}} = \{\mathcal{S}_j : \widetilde{P}_j > \gamma\} \quad \forall j \in \{1, \ldots, D\} \quad (4)$$

---

[1]For algorithm, see Section I-A of the supplementary material

where $\widetilde{S}$ denote the subset of source domains that meet the criterion $(\widetilde{P}_j > \gamma)$ and as consequence, are selected to updating the model Θ. For each subset $\widetilde{S}$ satisfying this condition, we compute a supervised loss as:

$$\mathcal{L}^s = -\frac{1}{\widetilde{D}} \frac{1}{N_s} \sum_{d=1}^{\widetilde{D}} \sum_{i=1}^{N_s} y_i^d \cdot \log(C(\mathbf{x}_i^d)) \qquad (5)$$

where $\widetilde{D}$ indicates the selected source subject domains. Note: After adapting $\mathbf{T}$ to the source domains included in $\widetilde{S}$, we update the pair-wise distances using Eq. 3 for the remaining source domains until we adapt the model Θ to the top_s closest source domains to the target domain.

C. Progressive Domain Adaptation of Target Subject

Following the P-MSDA paradigm of aligning a given domain, we have access to a sorted $\widetilde{S}$ comprised of source domains that are easy for the model Θ to align with the target. We gradually introduce source domains as $(\widetilde{S}_1, \mathbf{R}, \mathbf{T}; \Theta), (\widetilde{S}_2, \mathbf{R}, \mathbf{T}; \Theta), \ldots, (\widetilde{S}_D, \mathbf{R}, \mathbf{T}; \Theta)$. where Θ is the model that is updated at each step.

Density-based Selection of Samples in Replay Domain. We preserve the relevant samples from the adapted source subject to avoid the forgetting issue while introducing a new source domain into the adaptation process. To select samples for the replay domain, we create source $\widetilde{S}_a$ and target $\mathbf{T}$ clusters using density-based spatial clustering of applications with noise (DBSCAN) [59]. The samples are selected based on the closely related points of the source cluster $\mathbf{K}^s$ to the target cluster $\mathbf{K}^t$. We first estimate the local dense region of $\mathbf{K}^s$ by creating a matrix $\mathbf{H}^s \in \mathbb{F}^{K \times N^s}$, where K is the number of clusters, and N^s is the number of samples. Next, we calculate centroids $\mathbf{C}^s = \{\mathbf{c}_1^s, \mathbf{c}_2^s, \ldots, \mathbf{c}_K^s\}$ for each cluster, and estimate the Euclidean distance between each sample and centroid as:

$$\mathbf{H}_{j,i}^s = \left\| \mathbf{x}_i - \mathbf{c}_j \right\|^2 \quad \forall j \in \{1, \ldots, K\}, i \in \{1, \ldots, N^s\} \qquad (6)$$

where $\mathbf{H}_{j,i}^s$ consists of multiple distances computed from every j-th cluster. To pick the closest distance with the cluster centroids, we define:

$$Z^s = \min_{j \in \{1, \ldots, K\}} \{\mathbf{H}_{j,i}^s\} \quad \forall i \in \{1, \ldots, N^s\} \qquad (7)$$

where Z^s is a list of distances $\{z_1, z_2, \ldots, z_{N^s}\}$ sorted in ascending order to determine the closest samples to the cluster centroid. We sort the samples in $\widetilde{S}_a$ based on the distances in Z^s. Subsequently, to determine the distances of $\widetilde{S}_a$ from $\mathbf{T}$, we create target domain clusters $\mathbf{K}^t$ with centroids $\mathbf{C}^t = \{\mathbf{c}_1^t, \mathbf{c}_2^t, \ldots, \mathbf{c}_K^t\}$. The matrix $\mathbf{H}^t \in \mathbb{F}^{K \times N^t}$ is constructed, which calculates the Euclidean distance between the target domain clusters and source domain samples $\mathbf{x}^s$ using Eq. 6, and pick the closest samples using Eq. 7, which provide $Z^t = \{z_1, z_2, \ldots, z_{N^t}\}$ from $\mathbf{H}_{k,i}^t$. Note that here we do not sort Z^t, as the samples in $\widetilde{S}_a$ are already sorted according to $\mathbf{K}^s$, which corresponds to the dense region of the source domain. This helps eliminate outliers and ensures that we focus only on the most relevant part of the source.

Afterward, the top n distances from Z^t are selected and added to E. The updated distances are stored in $E = E \cup Z_{1:n}^t$. We now sort the distances in ascending order $E^* = Sort_{Asc}(E)$ while adding the relevant samples in $\mathbf{R}^* = \mathbf{R} \cup \mathbf{x}_{1:n}^s$. Based on E^*, we reorder all the samples $\mathbf{R}^* = \{\mathbf{x}_1^s, \mathbf{x}_2^s, \ldots, \mathbf{x}_{m+n}^s\}$, where m is the total number of existing data, n is the newly added samples. We then select the top N^r labeled examples:

$$\mathbf{R}^* = \{\mathbf{x}_i^r, y_i^r\}_{i=1}^{N^r} \qquad (8)$$

Thus, we estimate the loss of the replay-relevant domain as follows.

$$\mathcal{L}^r = -\frac{1}{N^r} \sum_{i=1}^{N^r} y_i^r \cdot \log(C(\mathbf{x}_i^r)) \qquad (9)$$

where $(\mathbf{x}^r, y^r)$, belongs to the updated replay domain $\mathbf{R}$, that re-calibrated after every $(\widetilde{S}, \mathbf{T})$ adaptation. Note that $\mathbf{R}$ is a dynamic domain that continues to update with the subset of source domains $\widetilde{S}$ [2].

Pseudo-label for Target Domain. To calculate the pseudo-labels for the target domain, motivated by the augmented confident pseudo-label (ACPL) technique presented in [18], we calculate the target labels by generating an augmented version $\widehat{\mathbf{x}}^t$ of each target sample $\mathbf{x}^t$ using a model Θ. We then estimate the probabilities as $\mathbf{p}^t = \text{softmax}(\mathbf{x}^t)$ and $\widehat{\mathbf{p}}^t = \text{softmax}(\widehat{\mathbf{x}}^t)$, taking the average of two probabilities $a^t = (\widehat{\mathbf{p}}^t + \mathbf{p}^t)/2$. The selection criteria to assign the pseudo-label to the target sample is determined by the confidence threshold τ based on $\tau = \tau_0 - \delta \lfloor \frac{e}{N} \rfloor$, where e the current epoch, N represents the epoch after which τ decreases, δ is the reduction value, and $\lfloor \cdot \rfloor$ is the floor function that rounded down to the nearest value. We assign the pseudo-labels to the target samples $\widehat{\mathbf{T}} = (\hat{\mathbf{x}}^t, \hat{y}^t)$ if a^t is greater than τ. At each training step, we estimate the target domain loss as:

$$\mathcal{L}^t = -\frac{1}{N^t} \sum_{i=1}^{N^t} \widehat{y}_i^t \cdot \log(C(\widehat{\mathbf{x}}_i^t)) \qquad (10)$$

Domain Alignment. We further mitigate the divergence between the domains using Maximum mean discrepancy (MMD) [60], which estimates the disparity among two distributions in RKHS space. In our problem, we have three subject domains $(\widetilde{S}_a, \widehat{\mathbf{T}}, \mathbf{R})$, we jointly calculate the pairwise distances between $(\widetilde{S}_a, \widehat{\mathbf{T}})$ and $(\widetilde{S}_a, \mathbf{R})$. For every new source, the disparity is calculated between the target domain, source domain, and replay domain which makes sure to eliminate the domain shift among them.

$$\mathcal{D}((\widetilde{S}, \widehat{\mathbf{T}}), (\widetilde{S}, \mathbf{R})) = \frac{1}{N^{s^2}} \sum_{i \neq j}^{N^s} k(\mathbf{x}_i^s, \mathbf{x}_j^s) + \frac{1}{N^{t^2}} \sum_{i \neq j}^{N^t} k(\mathbf{x}_i^t, \mathbf{x}_j^t)$$

$$-\frac{2}{N^s N^t} \sum_{i=1}^{N^s} \sum_{j=1}^{N^t} k(\mathbf{x}_i^s, \mathbf{x}_j^t) + \lambda \left\{ \frac{1}{N^{s^2}} \sum_{i \neq j}^{N^s} k(\mathbf{x}_i^s, \mathbf{x}_j^s) + \frac{1}{N^{r^2}} \sum_{i \neq j}^{N^r} k(\mathbf{x}_i^r, \mathbf{x}_j^r) \right\}$$

$$-\lambda \left\{ \frac{2}{N^s N^r} \sum_{i=1}^{N^s} \sum_{j=1}^{N^r} k(\mathbf{x}_i^s, \mathbf{x}_j^r) \right\} \qquad (11)$$

---

[2]The Algorithm is provided in Section I-B of the supplementary material

where $k(.,.)$ indicates a Gaussian kernel, while λ is the weight of the contribution of the samples from the replay domain. Thus, to reduce the domain disparity, the alignment loss is defined as

$$\mathcal{L}^{\text{dis}} = \sum_{d=1}^{\widetilde{D}} \mathcal{D}((\widetilde{\mathcal{S}}_a, \mathbf{T}), (\widetilde{\mathcal{S}}_a, \mathbf{R})) \qquad (12)$$

The $\mathcal{L}^{\text{dis}}$ is calculated for every a-th source domain that belongs to $\widetilde{D}$, i.e., only the selected source subjects. The total target adaptation loss is estimated as

$$\mathcal{L}^{\text{total}} = \mathcal{L}^{\text{s}} + \mathcal{L}^{\text{t}} + \mathcal{L}^{\text{r}} + \mathcal{L}^{\text{dis}} \qquad (13)$$

The final objective of our multi-subject domain adaptation of source selection is to minimize $\mathcal{L}^{\text{total}}$.

IV. EXPERIMENTAL METHODOLOGY

FER datasets, such as RAF-DB [61], or AffectNet [62] in the context of MSDA setting, often contain mixed individuals, that do not represent subject variations required to developed a subject-based adaptation method. Nevertheless, we evaluate our progressive MSDA technique for expression recognition on two widely used pain recognition datasets, Biovid part(A) [63], and UNBC-Master [64]. These datasets provide subject information with balanced class distributions, following the same experimental protocol established in [18]. Furthermore, we study the impact of gradually incorporating relevant source samples versus entire source subjects. It will elucidate the optimal strategy for enhancing performance and generalization capabilities in subject-based adaptation.

A. Datasets

BioVid Heat and Pain (PartA) [63] The dataset comprises 87 subjects recorded in a controlled environment, where each subject is categorized into one of five classes: "no pain" and four escalating pain levels labeled PA1 through PA4, representing increasing pain intensity. Previous studies have indicated that the lower pain intensities, particularly in the initial stages, did not elicit noticeable facial activities. It is recommended that the focus be on the "no pain" and highest pain intensity categories. Our experiments concentrate on two classes: "no pain" and the highest pain level, PA4. Each subject contributes 20 videos per class, lasting 5.5 seconds each. Following the findings in [65], which noted that PA4 does not display significant facial activity in the first 2 seconds of the video, we exclude frames from the initial 2 seconds. This ensures that only the latter part of the sequence, where the subject's response to pain is more pronounced, is analyzed.

UNBC-McMaster Shoulder Pain [64] comprises 25 subjects and includes 200 video sequences. Pain intensity for each frame is assessed using the PSPI scale [66], which ranges from 0 to 15. Given the substantial imbalance across pain intensity levels, we adopt the quantization strategy used in [67], where pain intensities are grouped into five discrete levels: 0 (no pain), 1 (intensity 1), 2 (intensity 2), 3 (intensity 3), 4 (intensities 4-5), and 5 (intensities 6-15).

B. Implementation Detail

In all experiments, we employ the ResNet18 backbone [68], which consists of the encoder F and the discriminative component C. To adapt F for subject-based MSDA, we follow the same protocol as [18] to remove the first ReLU, the MaxPool layers, and the final 2D adaptive average pooling layer. In our experiments, the backbone is shared across every domain, followed by the shared classifier. The images are resized to 100×100 resolution, and the model is trained with stochastic gradient descent (SGD) with a batch size of 16 and a learning rate of 10^{-4}. The closest source selection criterion is based on the threshold (τ), which is set to *0.8*, and the top_s is set to 40 subjects through empirical evaluation[3] . For generating target pseudo-labels we set a threshold based on $\theta = \theta_0 - \delta \left\lfloor \frac{e}{N} \right\rfloor$, the initial value of θ_0 is set to *0.91*, that was updated after every $N = 20$, with the reduction value δ is set to *0.01*. For the ACPL technique to generate reliable target PLs, we follow the same setting as Zeeshan et al. [18] and use a horizontal flip as an augmented version of the image. For replay relevant samples, we set top_n and N_r to 2000 samples, which are updated after each newly added source subject.

C. Baseline Methods

To evaluate the performance of our method, we define subjects as source and target domains. The first experiment was conducted on the BioVid dataset, where 77 subjects were treated as sources and adapted to the remaining ten target subjects. The following experiment is on the UNBC-McMaster dataset, which includes 20 subjects in the source domain adapted to the remaining five subjects in the target domain. To evaluate the efficacy of our model, we further experimented with a cross-dataset with 20 UNBC-McMaster sources adapted to 10 BioVid target subjects. We follow the previous work of Zeeshan et al. [18] to define the MSDA standard for pain recognition.

Source-combined: We first define the lower-bound, which is the traditional approach of training a model by using all the sources and testing the target subject. This approach is also known as source-only, as it does not adapt to the target data. The second experiment combines all subjects as before and then adapts to a target subject as in standard UDA.

Multi-source DA: We treat each subject as a separate domain while adapting to the target. We evaluated our method with three standard and one subject-based MSDA approaches moment matching for multi-source domain adaptation (M^3SDA) [35], implicit alignment (SImpAl) [37], contrastive multi-source domain adaptation (CMSDA), and subject-based domain adaptation [18]. M^3SDA technique was the baseline method for MSDA classification tasks that reduced the discrepancy based on the moment-matching approach between domains. CMSDA and SImpAI methods are based on generating the target PLs. Subject-based DA is the STA technique used in multi-source domain adaptation for pain estimation.

Oracle: It is the upper bound where we fine-tune the source model by leveraging labels of every target image in a fully supervised manner.

---

[3]Details are provided in Section III-B of the supplementary material.

TABLE I: Accuracy of our Subject-based MSDA and state-of-the-art methods on BioVid for ten target subjects with all 77 sources. **Bold** text shows the highest and *Italic* shows the second best accuracy.

Standards	Methods	Sub-1	Sub-2	Sub-3	Sub-4	Sub-5	Sub-6	Sub-7	Sub-8	Sub-9	Sub-10	Avg
Source Combine	Source-only	0.62	0.61	0.65	0.55	0.51	0.71	0.70	0.52	0.54	0.55	0.59
	Sub-based (UDA) [18]	0.73	0.64	0.73	0.59	0.54	0.75	0.76	0.53	0.51	0.58	0.63
Multi-Source	M^{3}SDA [35]	0.67	0.66	0.61	0.58	0.55	0.50	0.67	0.56	0.54	0.67	0.60
	CMSDA [20]	0.93	0.47	0.81	0.87	0.53	0.84	0.57	0.54	0.74	0.70	0.70
	SImpAI [37]	0.80	0.69	0.55	0.75	0.52	0.81	0.71	0.61	0.59	0.56	0.65
	Sub-based [18]	0.93	0.69	0.84	0.66	0.60	0.76	0.84	0.55	0.62	0.66	0.71
	Sub-based$_{top-k}$ [18]	0.93	0.71	**0.86**	0.87	0.88	0.92	0.86	0.77	0.84	0.68	0.83
	P-MSDA (ours)	**0.99**	**0.76**	**0.86**	**0.92**	**0.89**	**0.94**	**0.87**	**0.81**	**0.98**	**0.78**	**0.88**
Fully-Supervised	Oracle	0.99	0.91	0.98	0.97	0.98	0.97	0.96	0.95	0.99	0.98	0.96

TABLE II: Accuracy on UNBC-McMaster dataset of our method.

Methods	Sub-1	Sub-2	Sub-3	Sub-4	Sub-5	Avg
Source-only	0.74	0.84	0.81	0.68	0.83	0.78
Sub-based	0.76	0.87	0.84	0.70	0.85	0.80
M3SDA	0.78	0.87	0.92	0.66	0.81	0.80
CMSDA	0.80	0.86	0.83	0.71	0.85	0.81
SImpAI	0.80	0.88	0.81	0.70	0.87	0.81
Sub-based	0.81	0.91	**0.94**	0.72	0.92	0.86
P-MSDA	**0.87**	**0.93**	**0.94**	**0.74**	**0.94**	**0.88**
Oracle	0.96	0.98	0.97	0.94	0.97	0.96

V. RESULTS AND DISCUSSION

A. Comparison with State-of-the-Art

The result on the BioVid dataset is shown in Table I. In the source-only method, we follow the lower bound approach without any form of domain adaptation, where a model is trained on training subjects (sources) and evaluated on unlabeled target subjects. In the source-combined (blending) setting, we compare the result with the subject-based UDA method [18]. We compare our technique with four state-of-the-art MSDA methods. SImpAl, CMSDA, M^{3}SDA, and subject-based MSDA. Our method achieves higher performance for all target subjects with an average accuracy of *0.88* that exceeds the baseline by a large margin. The closest result was with a sub-based$_{top-k}$ with an average of *0.83* with a similar performance in *Sub-2* with *0.86* accuracy. Almost every model performance is impressive in subject *Sub-1*. However, our method yields remarkable performance in achieving the accuracy of *0.99*, which is the same as Oracle.

The result on UNBC-McMaster is presented in Table II. Our approach outperforms all methods on every target subject adaptation, including source-only and state-of-the-art MSDA methods, achieving an average accuracy of *0.88*, which is a gain from the previous subject-based method *0.86*. In particular, there is a significant improvement in *Sub-1* performance with an increase of *0.6* compared to the subject-based approach. For *Sub-3*, we match the performance with the subject-based method with *0.94* accuracy.

B. Cross-Dataset Evaluation

To further evaluate the efficacy of our method, we performed experiments on the cross-dataset setting, where we have 20 UNBC-McMaster labeled source subjects that were adapted to 10 unlabeled target subjects. The result for this setting is shown in Table III. We define the baseline as source-only, where the model is trained on source data and evaluated on the target test set. As expected, all the methods outperformed source-only; this is due to the significant domain shift between source and target domains. We further compare our method performance with three different MSDA approaches: SImpAI, CMSDA, and subject-based. Notably, all MSDA approaches demonstrate superior performance compared to the source-only model. This improvement can be attributed to their efficacy in mitigating discrepancies across diverse domains. However, for every target, our method achieves higher performance with an average accuracy of *0.78*, where the subject-based$_{top-k}$ matches the performance in *Sub-4* and *Sub-10* with accuracy *0.85* and *0.68*, respectively. It can be observed that MSDA techniques that neglect subject-specific feature representations often fail to optimize the model on the target subject. In contrast, our method demonstrates that choosing the relevant source subject is crucial for effective target adaptation, even when dealing with diversity in the source domain.

C. Impact of Progressive Adaptation on Source Domains

In this experiment, we further study the alternative approach to gradually learning by introducing the closest source samples instead of progressively introducing entire source domains. Fig. 6 (a) compares the effectiveness of selecting the closest source subjects with the closest source samples, random source samples, and the combination of all previously seen source subjects. Initially, we selected random source samples from all source domains and gradually introduced subsets of 2000 images, equivalent to the number of training images in a single subject from the BioVid dataset. The alternative approach is to select the closest samples from all source domains for each target based on cosine similarity. We gradually introduced these samples while retaining all previously seen samples. Our results indicate that this method improved performance

TABLE III: Cross-dataset evaluation: The source model is trained on UNBC-McMaster (20 subjects) and then adapted to 10 BioVid target subjects.

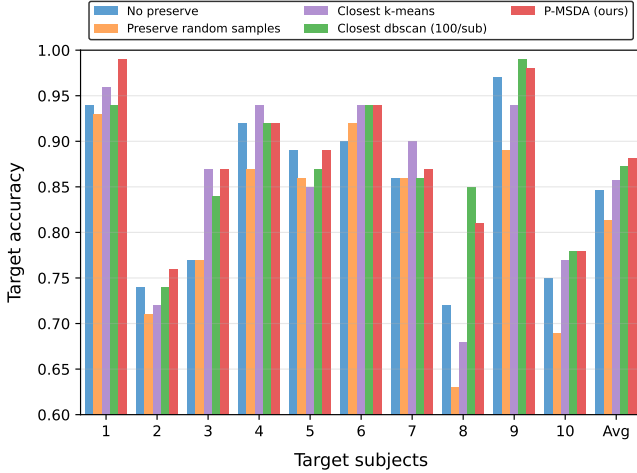| Methods	Sub-1	Sub-2	Sub-3	Sub-4	Sub-5	Sub-6	Sub-7	Sub-8	Sub-9	Sub-10	Avg
Source-only	0.81	0.54	0.48	0.61	0.52	0.63	0.50	0.48	0.57	0.54	0.56
SImpAI	0.87	0.64	0.67	0.66	0.58	0.81	0.69	0.53	0.71	0.59	0.67
CMSDA	0.88	0.61	0.69	0.55	0.52	0.79	0.63	0.52	0.77	0.67	0.66
Sub-based	0.90	0.50	0.52	0.69	0.50	0.52	0.53	0.50	0.50	0.58	0.57
Sub-based$_{top-k}$	0.84	0.57	0.50	**0.85**	0.72	0.78	0.52	0.52	0.53	**0.68**	0.65
P-MSDA (Ours)	**0.90**	**0.66**	**0.80**	**0.85**	**0.86**	**0.86**	**0.73**	**0.54**	**0.94**	**0.68**	**0.78**

Fig. 3: Analysis of different techniques to select the relevant samples for the replay domain. *No Preserve*, at each increment step we only use the new subject without considering previously visited samples; *Preserve Random Samples*, select fixed random samples from previous domains; *Closest k-means*, select samples based on k-means clusters; *Closest DBSCAN (100/subject)*, incorporate 100 samples from each visited source subject using DBSCAN; *Ours*, density-based selection of pertinent samples.

compared to randomly selecting source samples. Nevertheless, the model performed even better when introducing the closest subjects. This improvement can be attributed to preserving subject-specific features that maintain the contextual information within the same subject, which helped the model learn more consistent representations relevant to each target. While training with all closest subjects and accumulating previously visited subjects initially outperformed the other approaches. However, as more subjects were included over time, there was less focus on newer subjects, resulting in minimal gains in adaptation performance. On the other hand, when only training with the closest source subjects and retaining the most relevant previous samples, performance improved significantly over time. This approach also required less memory and computational resources since it did not involve saving all previously seen data, leading to faster convergence.

D. Impact of Gradually Introducing Source Domains

We investigate the impact of gradually adding source domains on transfer loss, defined as the discrepancy between

source and target domains. This experiment was conducted using the BioVid dataset, with target *Sub-10*. Fig. 6 (b) illustrates the impact of transfer loss as new sources are introduced. It can be seen that when we added a new source domain, there was a spike in the loss due to the variability between subjects. Following each spike, the model demonstrates its ability to minimize the discrepancy between domains, as evidenced by the subsequent reduction in transfer loss. Furthermore, as training progressed and new subjects were incorporated, we observed a consistent downward trend in transfer loss. This pattern suggests effective model convergence of the selective target subject.

E. Impact of Approaches to Preserve Samples for Replay Domain

To evaluate the efficacy of our proposed approach, we conducted an extensive ablation study on the BioVid dataset, comparing various techniques to select relevant samples for the replay domain, illustrated in Fig. 3. We analyze performance across five different settings: *No Preserve*, *Preserve Random Samples*, *Closest K-means*, *Closest DBSCAN (100/subject)*, and *Ours*, In *No Preserve* setting, we introduce a new source subject to the target without preserving any previous samples. At each introduction of the source subject, the model only relies on the current subject, which raises the forgetting issue and affects the adaptation process *Preserve Random Samples*, we randomly select and retain 2,000 samples from previous sources. This selection criterion performed the worst as compared to other techniques because the model fails to capture subject-specific features crucial for the target subject. This indicates that the model exhibits high sensitivity to person-specific characteristics. Thus, when presented with samples that deviate significantly from the target subject, the model struggles to adapt effectively. This highlights the importance of the sample selection strategy. Next, In *Closest K-means*, we employ the K-means clustering algorithm to identify and select the most relevant data points. Overall, the results from the previous technique are improved. However, in K-means, it is required to define the number of clusters, and its sensitivity to the outliers may limit its efficacy in selecting the most pertinent samples. *Closest DBSCAN (100/subject)*, which utilizes the Density-Based Spatial Clustering of Applications with Noise (DBSCAN) algorithm to select 100 samples from each source subject. This approach demonstrates a significant improvement over K-means, primarily due to its ability to form clusters based on density measures without requiring
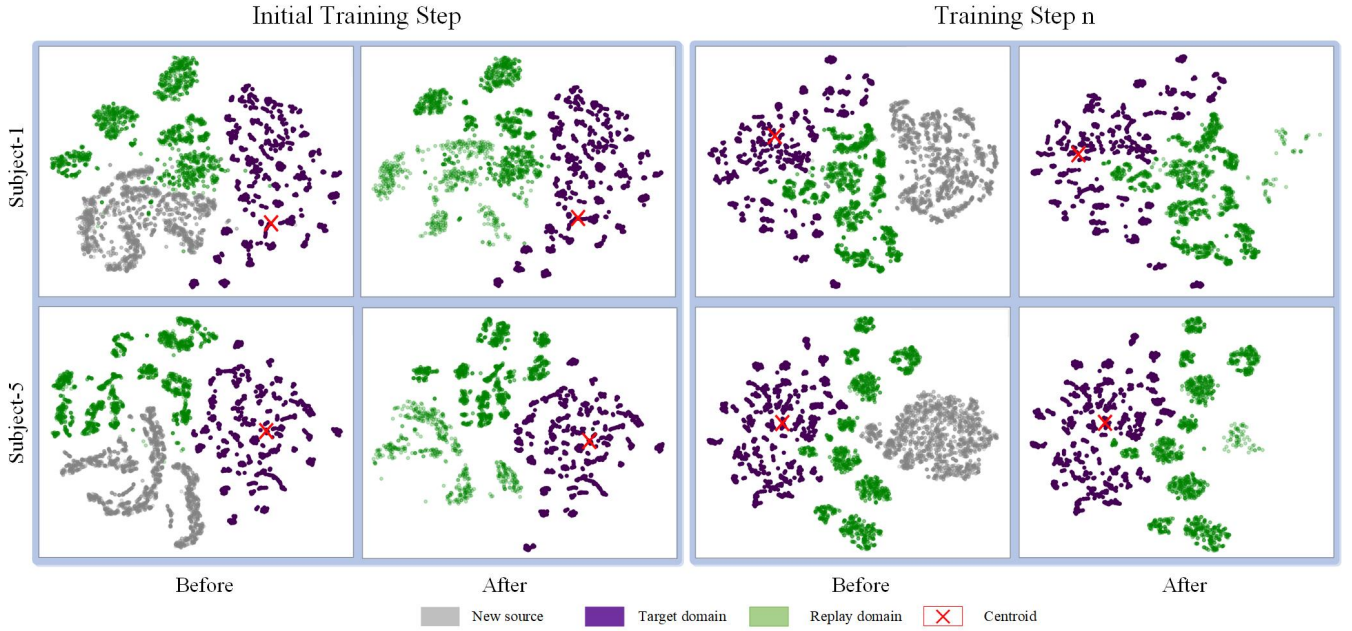
Fig. 4: T-SNE visualization of patterns from Biovid on source domain, replay domain, and the target domain (*Subject-1* and *Subject-5*). We illustrate how the replay domain preserves samples over different training steps. Before and after, embeddings of selecting pertinent features from the new source subject were extracted. *Initial Step* preserves more samples from the source. *Step n*, incorporate fewer samples from later sources, it minimizes the influence of distant subjects while enhancing alignment with the target.
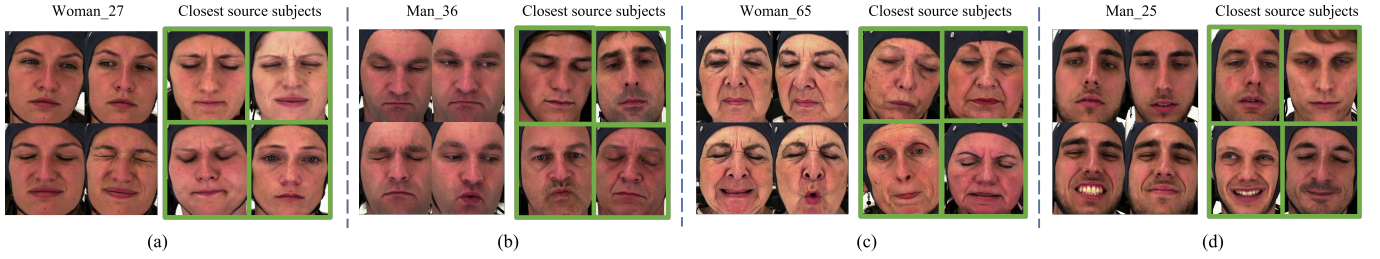

Fig. 5: Selection of closest source subjects. Example of unlabeled target subject: (a) *Woman 27 (Sub-1)*, (b) *Man 36 (Sub-2)*, (c) *Woman 65 (Sub-9)*, and (d) *Man 25 (Sub-6)* and their respective top-ranked selected source subjects.
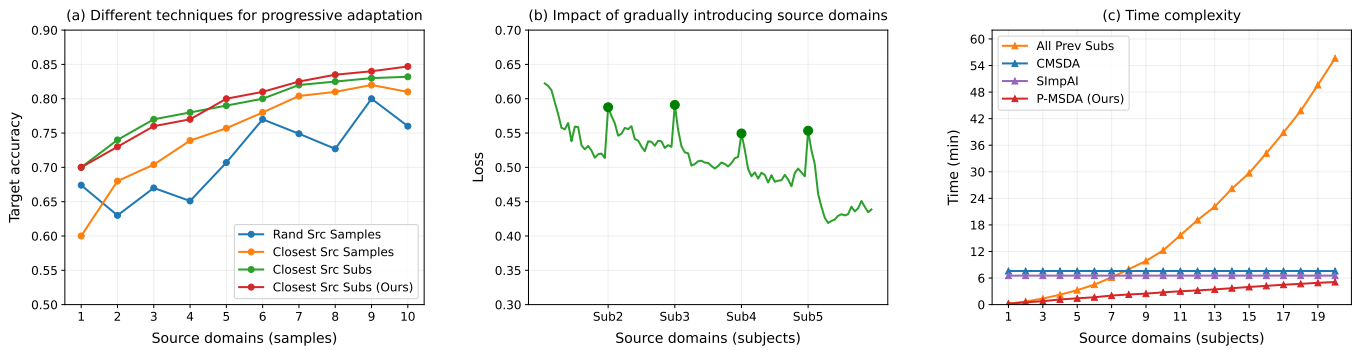

Fig. 6: (a) We compare four techniques to gradually introduce source data; i) *Random Source Samples*, ii) *Closest Source Samples*, iii) *Closest Source Subjects (all)*, and iv) *Closest Source subjects (ours)*. Every point represents an average of all the target subjects in BioVid. On the x-axis, each increment is equivalent to approximately. 2k samples or a single subject. (b) Loss when introducing a new source domain, adapting to BioVid target subject-10. (c) Time complexity comparison for training; All Previous Subjects, CMSDA, SImpAI, and P-MSDA (ours).

predefined clusters while effectively eliminating outliers. This aligns with our objective of selecting samples closer to the centroid and avoiding outliers without prior knowledge of cluster numbers. Finally, our proposed method applies DBSCAN to create a density-based dictionary that stores the most relevant samples, eliminating the fixed per-subject sample selection.

This highlights the importance of selecting the most expressive samples while avoiding the inclusion of potentially irrelevant samples from all source subjects.

F. Visualization

Density-based Selection of Replay Domain. Fig. 4 illustrates a t-SNE [69] representation of the embeddings from the last layer of the feature extractor $F(.)$ on Biovid target *Subject-1* and *Subject-5*. We show the latent space of the features from a density-based selection of the replay domain before and after selecting a pertinent sample from a new source subject while adapting to a target subject. In the initial training step, the model retains more samples from the newly added source, as the network is more flexible in the initial stage, allowing more relevant samples to be included in a replay dictionary. On the other hand, as training progresses to step n, the replay dictionary is less affected by the newly added source subject. Two notable observations can be made here. First, the model gradually acquires useful knowledge from earlier subjects that are more closely related to the target, resulting in fewer samples being drawn from later sources, thereby minimizing the influence of more distant subjects. Second, the samples within the replay dictionary become tightly clustered with the target features, improving alignment with the target domain. **Selection of Relevant Source Domains.** Fig. 5 illustrates an example of four target subjects: *Woman 27 (Sub-1)*, *Man 36 (Sub-2)*, *Woman 65 (Sub-9)*, and *Man 25 (Sub-6)* with their respective closest source subjects (using cosine similarity) that are structurally more similar. These subjects are selected first to optimize the model for target adaptation.

G. Complexity Analysis

Fig. 6 (c) presents the convergence time of the model to the target domain as the number of source domains increases incrementally. This experiment is conducted on the BioVid dataset, using 20 source domains and adapting to the target domain *sub-4*, with training performed for one epoch on an NVIDIA A100 GPU. We evaluate the time complexity across four approaches: **All Previous Subjects**, **CMSDA**, **SImpAI**, and **P-MSDA (ours)**. In the All Previous Subjects method, all previously visited source domains are retained while progressively adding new ones, making it computationally expensive due to including all subjects at each step. In contrast, CMSDA and SImpAI integrate all source domains at the start of training. As these methods do not involve gradual adaptation, their time complexity is measured after processing all 20 source domains, resulting in a fixed time complexity regardless of the number of included domains. Our proposed approach, P-MSDA, maintains a constant number of three domains source, target, and replay throughout training. Gradual adaptation is achieved by replacing the current source with a new one and updating the replay domain with previously visited sources. During target adaptation, our method operates with $d=3$ domains and approximately $n=2000$ samples per domain, resulting in a total sample size $N = n \cdot d$. Training for one epoch takes approximately $t=15 \cdot d$ seconds. In the All Previous Subjects method, each addition of a new source

domain increases the total sample size to $N^*=n \cdot (d+1)$, leading to a proportional rise in training time to $t^*=t \cdot (d+1)$. However, our method ensures stable training complexity by consistently maintaining $d=3$ domains.

VI. CONCLUSION

We proposed a novel method of progressively selecting source subjects for personalized facial expression recognition in multi-source domain adaptation. Our model allows the most relevant source subjects to gradually adapt to a target individual in a curriculum manner while preserving the most pertinent samples from the visited sources for the replay domain. We evaluated the efficacy of our model by comparing two scenarios of within and cross-dataset settings. i) for BioVid and UNBC-McMaster, performance is improved significantly for all 10 and 5 target subjects, respectively; ii) For UNBC-McMaster (source) → BioVid (target), where subjects are from different domains, our model still outperformed other techniques. Furthermore, we performed a comprehensive analysis of the importance of selecting relevant previous source samples. This enables maintaining important characteristics while adapting to a target subject.

VII. ALGORITHMS

A. Selection of Source Domains

Algorithm 1 shows the selection of source domains for target adaptation. Initially, we prioritize the source domains with high transferability to align them with the target domain. This will help select source domains with feature distributions similar to the target domain. After aligning the feature distributions of these source domains, a source selection will prioritize the next round of source domains for alignment. As adaptation (training) continues, the model gradually learn to focus on various aspects of the feature distribution to improve transferability. Our approach involves learning a curriculum to prioritize different source domains.

B. Density-based Selection of Replay Domain

Algorithm 2 shows our method for *density-based selection of samples in replay domain*. We preserve the relevant samples from the adapted source subject to avoid the forgetting issue while introducing a new source domain into the adaptation process.

VIII. ADDITIONAL IMPLEMENTATION DETAIL

Our method is implemented on PyTorch [70]. For the training of source and target domain subjects, we selected a batch size of 16 with a momentum of 0.9. The learning rate was set to 0.0001, whereas the learning rate between linear and classification layers was set to 0.001. SGD optimizer

Algorithm 1 Source Selection for Target Adaptation

Require:
   $\mathcal{S}$: set of labeled source domains
   T: unlabeled target domain
   γ: threshold
   top_s: number of top source domains
   Initialize: $P \leftarrow []$ # List to store domain distances
   Initialize: $V \leftarrow []$ # List of adapted (visited) sources
   Initialize $\mathbf{R} \leftarrow \emptyset$ ▷ **R** is a replay domain for $(\mathbf{x}, y)$ pairs
1: **while** $|V| < top_s$ **do**
2:     Filter $\mathcal{S}$ to get domains that are not yet adapted
3:     **for** each domain $\mathbf{S}_a$ in $\mathcal{S}$ **do**
4:         Compute cosine similarity p_a in mini-batch between samples in $\mathbf{S}_a$ and **T** 3
5:         Append calculated p_a to P
6:     **end for**
7:     Obtain $\widetilde{P}$ by normalizing P between range $[0-1]$
8:     Select the closest $\widetilde{\mathcal{S}}$ using $\widetilde{P}$ and γ by (4)
9:     Append $\widetilde{\mathcal{S}}$ to V
10:     **for** each $\widetilde{\mathbf{S}}_a \in \widetilde{\mathcal{S}}$ **do**
11:         Compute $\mathcal{L}^s$ for $\widetilde{\mathbf{S}}_a$
12:         Compute $\mathcal{L}^t$ for **T**
13:         # Initially when R is ∅, assign $\widetilde{\mathbf{S}}_a$
14:         $\mathbf{R} \leftarrow \mathbf{R} = \emptyset$? $\widetilde{\mathbf{S}}_a$: $\mathbf{R}$
15:         Compute $\mathcal{L}^r$ for **R**
16:         Compute $\mathcal{L}^{dis}$ for $\widetilde{\mathbf{S}}_a$, **T**, and **R**
17:         $\mathbf{R} \leftarrow$ **Algorithm 2**$(\widetilde{\mathbf{S}}_a, \mathbf{T}, \mathbf{R})$ # Update R
18:     **end for**
19: **end while**

Algorithm 2 Density-based Selection of Samples in Replay Domain

Require:
   $\widetilde{\mathbf{S}}_a$: selected source domain
   T: unlabeled target domain
   R: replay relevant domain
Ensure: Updated replay relevant samples $\mathbf{R}^*$
   Initialize: $E \leftarrow []$ # List to store distances
   Initialize: $Z^s \leftarrow []$, $Z^t \leftarrow []$ # List to store samples
   Initialize: Create clusters $\mathbf{K}^s$ and $\mathbf{K}^t$ using embeddings from $\widetilde{\mathbf{S}}_a$ and **T** to compute centroids $\mathbf{C}^s$ and $\mathbf{C}^t$
1: **for** each $\mathbf{x}^s \in \widetilde{\mathbf{S}}_a$ **do**
2:     Compute $\mathbf{H}^s_{\mathbf{k},\mathbf{i}}$ as distances to $\mathbf{C}^s$ by (6)
3:     Construct Z^s by selecting the closest samples (7)
4: **end for**
5: $\hat{Z}^s \leftarrow Sort_{Asc}(Z^s)$
6: Reorder $\widetilde{\mathbf{S}}_a$ based on $\hat{Z}^s$
7: **for** each $\mathbf{x}^s \in \widetilde{\mathbf{S}}_a$ **do**
8:     Compute $\mathbf{H}^t_{\mathbf{k},\mathbf{i}}$ as distances to $\mathbf{C}^t$ by (6)
9:     Construct Z^t by selecting the closest samples (7)
10: **end for**
11: Update $E^* \leftarrow E \cup Z^t_{1:n}$ and sort
12: Append top samples to $\mathbf{R}^* \leftarrow \mathbf{R} \cup \mathbf{x}^s_{1:n}$
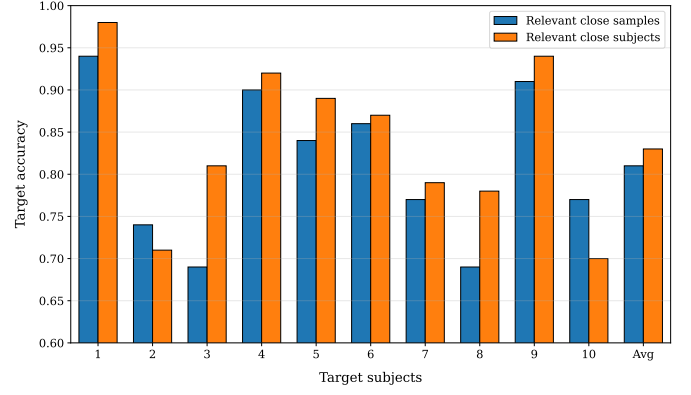13: Select top N^r examples by (8)
14: **return** $\mathbf{R}^*$

Fig. 7: Comparison between selecting closest samples versus selecting closest subjects.

is chosen with the weight decay of 5e-4. In the training of source subjects, the value of trade-off parameter λ is set to 0.1. For the source selection, we set the threshold to *0.90*. The selected source domains are used for the target adaptation, then the next batch of sources were calculated, and the adaptation process will continue until it reaches top_s which is set to 40 subjects, empirically see section V-F. **Target Subjects:** To make it consistent and comparable across all of our experiments. We select 10 fixed target subject domains from the BioVid Heat Pain Dataset [63]. To have a better target adaptability, we did not select any of the subjects that belong to the 20 unexpressed individuals as cited in [65]. These subjects are: `081014_w_27`, `101609_m_36`, `112009_w_43`, `091809_w_43`, `071309_w_21`, `073114_m_25`, `080314_w_25`, `073109_w_28`, `100909_w_65`, `081609_w_40`. For UNBC-McMaster we selected 5 target subjects: `107-hs107`, `109-ib109`, `121-vw121`, `123-jh123`, `115-jy115`. For cross-dataset, we use same 10 target subjects from Biovid.

IX. ABLATIONS

A. Impact of Selection of Source Domain

In this ablation, we study different ways of selecting source subjects that are closer to the target domain in the BioVid dataset, shown in Table IV. In *N-Classes*, we train a ResNet18 model on the 'N' number of classes, where 'N' is the number of source subjects, i.e., 77. The model is trained for 20 epochs, where each class is associated with a source subject. After training, we introduce a target subject to make a prediction. The class with the highest prediction rate will be closest to the target subject. Therefore, we rank the subjects from the highest to the lowest prediction and adapt to the target subject sequentially. This method matches the performance of *Sub-4* with other techniques, achieving an average accuracy of *0.83*. The following criterion was estimating the distance of sources with the target by the maximum mean difference (MMD), improving performance by *0.4*. Finally, when we apply cosine-similarity, it exceeds the other two methods by converging to every target subject, significantly improving the adaptation rate.

TABLE IV: Different source selection criteria. *N-Classes*, determine by training a *N* source classes; *Maximum Mean Discrepancy (MMD)*, select closest sources from the target; *Cosine-Similarity (CoS)*, pick based on the similarity score.

Source Selection	Sub-1	Sub-2	Sub-3	Sub-4	Sub-5	Sub-6	Sub-7	Sub-8	Sub-9	Sub-10	Avg
N-Classes	0.94	0.72	0.78	**0.92**	0.87	0.87	0.87	0.64	0.97	0.76	0.83
MMD	0.97	0.75	0.83	**0.92**	0.86	**0.94**	**0.90**	0.81	0.98	0.75	0.87
CoS	**0.99**	**0.76**	**0.86**	**0.92**	**0.89**	**0.94**	0.87	**0.81**	**0.98**	**0.78**	**0.88**

TABLE V: Selecting Top_s value for the selection of source domains

Top_s	Sub-1	Sub-2	Sub-3	Sub-4	Sub-5	Sub-6	Sub-7	Sub-8	Sub-9	Sub-10	Avg
Top-10	0.90	0.58	0.78	0.91	**0.89**	0.91	0.84	0.74	0.76	0.65	0.796
Top-20	0.96	0.64	0.81	**0.92**	0.83	0.92	**0.87**	**0.81**	0.97	0.74	0.847
Top-30	0.95	0.65	0.78	0.90	0.83	0.92	0.78	0.72	**0.98**	0.70	0.821
Top-40	**0.99**	0.73	**0.87**	0.92	0.88	**0.94**	0.80	0.81	0.94	**0.78**	0.866
Top-50	0.96	0.73	0.82	0.87	0.79	0.93	0.82	0.73	0.94	0.77	0.836
Top-60	0.95	0.72	0.61	0.90	0.81	0.90	0.79	0.61	0.85	0.71	0.785
Top-70	0.90	**0.76**	0.81	0.91	0.49	0.85	0.80	0.68	0.51	0.72	0.743
All subjects (77)	0.68	0.69	0.78	0.84	0.65	0.90	0.83	0.72	0.51	0.71	0.731

B. Choosing Top-s Value for Source Domain Selection

The closest source selection criterion is based on the τ, which is set to *0.80*, and the top_s is set to 40 for Biovid subjects (except for sub-2). For UNBC-McMaster, the total number of source subjects is 20, selecting top_s to 20 subjects. Table V shows empirically the selection criteria of Top_s value. The experiment demonstrates the convergence of the proposed method, with 9 out of 10 target subjects achieving convergence within the first 40 source subjects (Top_s = 40). *Sub-2* displayed a delayed convergence, which required additional sources to reach stability. This outlier behavior indicates domain-specific characteristics present in the *Sub-2* data distribution, requiring more sources of information for the convergence.

C. Visualization of Density-based Selection of Relevant Samples

Fig. 4 illustrates a t-SNE [69] representation of the embeddings from the last layer of the feature extractor $F(.)$ on Biovid target *Subject-1* and *Subject-5*. We show the latent space of the features from a density-based selection of the replay domain before and after selecting a pertinent sample from a new source subject while adapting to a target subject. In the initial training step, the model retains more samples from the newly added source, as the network is more flexible in the initial stage, allowing more relevant samples to be included in a replay dictionary. On the other hand, as training progresses to step n, the replay dictionary is less affected by the newly added source subject. Two notable observations can be made here. First, the model gradually acquires useful knowledge from earlier subjects that are more closely related to the target, resulting in fewer samples being drawn from later sources, thereby minimizing the influence of more distant subjects. Second, the samples within the replay dictionary become tightly clustered with the target features, improving alignment with the target domain.

REFERENCES

[1] M. H. Aslam et al., "Privileged knowledge distillation for dimensional emotion recognition in the wild," in *CVPR workshops*, 2023.

[2] M. Sharafi et al., "Disentangled source-free personalization for facial expression recognition with neutral target data," *CoRR*, vol. abs/2503.20771, 2025.

[3] M. H. Aslam and M. O. Zeeshan et al., "Distilling privileged multimodal information for expression recognition using optimal transport," in *FG*, 2024.

[4] P. Waligora et al., "Joint multimodal transformer for emotion recognition in the wild," in *CVPR workshops*, 2024.

[5] S. Ben-David et al., "A theory of learning from different domains," *Machine learning*, 2010.

[6] M. Rescigno et al., "Personalized models for facial emotion recognition through transfer learning," *Multimedia Tools and Applications*, 2020.

[7] P. Barros, G. Parisi, and S. Wermter, "A personalized affective memory model for improving emotion recognition," in *ICML*, 2019.

[8] G. Zen, L. Porzi, E. Sangineto, E. Ricci, and N. Sebe, "Learning personalized models for facial expression analysis and gesture recognition," *IEEE Transactions on Multimedia*, 2016.

[9] S. Ren, K. He, R. Girshick, and J. Sun, "Faster r-cnn: Towards real-time object detection with region proposal networks," *NeurIPS*, 2015.

[10] J. Hu, L. Shen, and G. Sun, "Squeeze-and-excitation networks," in *CVPR*, 2018.

[11] A. Gretton et al., "A kernel two-sample test," *The Journal of Machine Learning Research*, 2012.

[12] M. Long, H. Zhu, J. Wang, and M. I. Jordan, "Unsupervised domain adaptation with residual transfer networks," *NeurIPS*, 2016.

[13] J. Han, L. Xie, J. Liu, and X. Li, "Personalized broad learning system for facial expression," *Multimedia Tools and Applications*, 2020.

[14] S. Li and W. Deng, "Deep emotion transfer network for cross-database facial expression recognition," in *ICPR*, 2018.

[15] R. Zhu, G. Sang, and Q. Zhao, "Discriminative feature adaptation for cross-domain facial expression recognition," in *ICB*, 2016.

[16] S. Zhao, B. Li, and P. Xu et al., "Madan: multi-source adversarial domain aggregation network for domain adaptation," *IJCV*, 2021.

[17] S. Zhao et al., "Multi-source distilling domain adaptation," in *AAAI*, 2020.

[18] M. O. Zeeshan et al., "Subject-based domain adaptation for facial expression recognition," in *FG*, 2024.

[19] G. Kang et al., "Contrastive adaptation network for single-and multi-source domain adaptation," *TPAMI*, 2020.

[20] M. Scalbert et al., "Multi-source domain adaptation via supervised contrastive learning and confident consistency regularization," *CoRR*, vol. abs/:2106.16093, 2021.

[21] M. T. Rosenstein, Z. Marx, L. P. Kaelbling, and T. G. Dietterich, "To transfer or not to transfer," in *NIPS 2005 workshop on transfer learning*, 2005.

[22] Z. Wang, Z. Dai, B. Póczos, and J. Carbonell, "Characterizing and avoiding negative transfer," in *CVPR*, 2019.

[23] Y. Bengio, J. Louradour, R. Collobert, and J. Weston, "Curriculum learning," in *ICML*, 2009.

[24] M. Kumar, B. Packer, and D. Koller, "Self-paced learning for latent variable models," *NeurIPS*, 2010.

[25] M. De Lange et al., "Continual learning: A comparative study on how to defy forgetting in classification tasks," *CoRR*, vol. abs/1909.08383, 2019.

[26] G. I. Parisi et al., "Continual lifelong learning with neural networks: A review," *Neural networks*, 2019.

[27] R. Aljundi, P. Chakravarty, and T. Tuytelaars, "Expert gate: Lifelong learning with a network of experts," in *CVPR*, 2017.

[28] I. A. Laurensi et al., "Alleviating catastrophic forgetting in facial expression recognition with emotion-centered models," in *ICPR*, 2024.

[29] D. Isele and A. Cosgun, "Selective experience replay for lifelong learning," in *AAAI*, 2018.

[30] M. Ghifary et al., "Deep reconstruction-classification networks for unsupervised domain adaptation," in *ECCV*, 2016.

[31] J.-Y. Zhu et al., "Unpaired image-to-image translation using cycle-consistent adversarial networks," in *ICCV*, 2017.

[32] T. Chen et al., "Cross-domain facial expression recognition: A unified evaluation benchmark and adversarial graph learning," *TPAMI*, 2021.

[33] A. Odena et al., "Conditional image synthesis with auxiliary classifier gans," in *ICML*, 2017.

[34] K. Yan et al., "Unsupervised facial expression recognition using domain adaptation based dictionary learning approach," *Neurocomputing*, 2018.

[35] X. Peng et al., "Moment matching for multi-source domain adaptation," in *ICCV*, 2019.

[36] V.-A. Nguyen et al., "Stem: An approach to multi-source domain adaptation with guarantees," in *ICCV*, 2021.

[37] N. Venkat, J. N. Kundu, D. Singh, A. Revanur *et al.*, "Your classifier can secretly suffice multi-source domain adaptation," *NeurIPS*, 2020.

[38] Z. Deng, D. Li, Y.-Z. Song, and T. Xiang, "Robust target training for multi-source domain adaptation," *CoRR*, vol. abs/:2210.01676, 2022.

[39] S. Zhou et al., "Active gradual domain adaptation: Dataset and approach," *IEEE Transactions on Multimedia*, 2022.

[40] H.-Y. Chen and W.-L. Chao, "Gradual domain adaptation without indexed intermediate domains," *NeurIPS*, 2021.

[41] H. Wang et al., "Understanding gradual domain adaptation: Improved analysis, optimal path and beyond," in *ICML*, 2022.

[42] S. Abnar et al., "Gradual domain adaptation in the wild: When intermediate distributions are absent," *CoRR*, vol. abs/:2106.06080, 2021.

[43] Y. Hsu et al., "Re-evaluating continual learning scenarios: A categorization and case for strong baselines. continual learning workshop," in *NeurIPS*, 2018.

[44] M. De Lange et al., "A continual learning survey: Defying forgetting in classification tasks," *TPAMI*, 2021.

[45] Z. Mai et al., "Online continual learning in image classification: An empirical survey," *Neurocomputing*, 2022.

[46] M. J. Mirza et al., "An efficient domain-incremental learning approach to drive in all weather conditions," in *CVPR*, 2022.

[47] U. Michieli and P. Zanuttigh, "Incremental learning techniques for semantic segmentation," in *ICCV workshops*, 2019.

[48] J. Xu and Z. Zhu, "Reinforced continual learning," *NeurIPS*, 2018.

[49] S. Hou, X. Pan, C. C. Loy, Z. Wang, and D. Lin, "Learning a unified classifier incrementally via rebalancing," in *CVPR*, 2019.

[50] J. Zhang et al., "Class-incremental learning via deep model consolidation," in *WACV*, 2020.

[51] H. Shin, J. K. Lee, J. Kim, and J. Kim, "Continual learning with deep generative replay," *NeurIPS*, 2017.

[52] X. Wei et al., "Incremental learning based multi-domain adaptation for object detection," *Knowledge-Based Systems*, 2020.

[53] M. Kiran et al., "Incremental multi-target domain adaptation for object detection with efficient domain transfer," *PR*, 2022.

[54] J. Choi, M. Jeong, T. Kim, and C. Kim, "Pseudo-labeling curriculum for unsupervised domain adaptation," *CoRR*, vol. abs/:1908.00262, 2019.

[55] Z. Wang, C. Zhou, B. Du, and F. He, "Self-paced supervision for multi-source domain adaptation." in *IJCAI*, 2022.

[56] L. Jiang, D. Meng, Q. Zhao, S. Shan, and A. Hauptmann, "Self-paced curriculum learning," in *AAAI*, 2015.

[57] L. Yang, Y. Balaji, S.-N. Lim, and A. Shrivastava, "Curriculum manager for source selection in multi-source domain adaptation," in *ECCV*, 2020.

[58] A. K. Mondal, V. Jain, and K. Siddiqi, "Mini-batch similarity graphs for robust image classification." in *BMVC*, 2021.

[59] M. Ester, H.-P. Kriegel, J. Sander, X. Xu *et al.*, "A density-based algorithm for discovering clusters in large spatial databases with noise," in *kdd*, 1996.

[60] D. Sejdinovic, B. Sriperumbudur, A. Gretton, and K. Fukumizu, "Equivalence of distance-based and rkhs-based statistics in hypothesis testing," *The annals of statistics*, 2013.

[61] S. Li, W. Deng, and J. Du, "Reliable crowdsourcing and deep locality-preserving learning for expression recognition in the wild," in *CVPR*, 2017.

[62] D. Kollias et al., "Deep affect prediction in-the-wild: Aff-wild database and challenge, deep architectures, and beyond," *IJCV*, 2019.

[63] S. Walter et al., "The biovid heat pain database data for the advancement and systematic validation of an automated pain recognition system," in *CYBCO*, 2013.

[64] P. Lucey et al., "Painful data: The unbc-mcmaster shoulder pain expression archive database," in *FG*, 2011.

[65] P. Werner, A. Al-Hamadi, and S. Walter, "Analysis of facial expressiveness during experimentally induced heat pain," in *ACIIW*. IEEE, 2017.

[66] K. M. Prkachin, "The consistency of facial expressions of pain: a comparison across modalities," *Pain*, vol. 51, no. 3, pp. 297–306, 1992.

[67] G. P. Rajasekhar et al., "Deep domain adaptation with ordinal regression for pain assessment using weakly-labeled videos," *Image and Vision Computing*, 2021.

[68] K. He, X. Zhang, S. Ren, and J. Sun, "Deep residual learning for image recognition," in *CVPR*, 2016.

[69] L. Van der Maaten and G. Hinton, "Visualizing data using t-sne." *Journal of machine learning research*, 2008.

[70] A. Paszke, S. Gross, F. Massa, A. Lerer, J. Bradbury, G. Chanan, T. Killeen, Z. Lin, N. Gimelshein, L. Antiga *et al.*, "Pytorch: An imperative style, high-performance deep learning library," *Advances in neural information processing systems*, vol. 32, 2019.

Muhammad Osama Zeeshan received a Bachelors degree in Computer Sciences from Air University Islamabad and a Masters degree in Data Sciences from Bahria University Islamabad. He is currently pursuing his Doctoral Degree in System Engineering from École de Technologie Supérieure (ÉTS) Montreal, Canada. His research interests include deep learning, computer vision, pattern recognition, unsupervised domain adaptation, and affective computing.

Marco Pedersoli is associate professor at ETS Montreal. He obtained his PhD in computer science in 2012 at the Autonomous University of Barcelona and the Computer Vision Center of Barcelona. At ETS Montreal he is a member of LIVIA and ILLS and he is co-chairing an industrial Chair on Embedded Neural Networks for Connected Building Control. His research is mostly applied on visual recognition, the automatic interpretation and understanding of images and videos. His specific focus is on reducing the complexity and the amount of annotation required for deep learning algorithms such as convolutional and recurrent neural networks. Prof. Pedersoli has authored more than 50 publications in top-tier international conferences and journals in computer vision and machine learning.

Alessandro Lameiras Koerich (Member, IEEE) received the Ph.D. degree in engineering from the École de Technologie Supérieure (ÉTS), in 2002. He is currently a professor at the Department of Software and IT Engineering, ÉTS, University of Québec, Montreal. His current research interests include multimodal and trustworthy machine learning and affective computing. He is an associate editor of the IEEE Transactions on Affective Computing, Pattern Recognition, and Expert Systems with Applications. He has served as the general chair of the 14th International Society for Music Information Retrieval Conference, which was held in Curitiba, Brazil, in 2013. In 2004, he was nominated as an IEEE CS Latin America Distinguished Speaker.

Eric Granger (Member, IEEE) received the Ph.D. degree in EE from École Polytechnique de Montréal in 2001. He was a Defense Scientist with DRDC, Ottawa, from 1999 to 2001, and in Research and Development with Mitel Networks from 2001 to 2004. He joined the Department of Systems Engineering, École de technologie supérieure, Montreal, Canada, in 2004, where he is currently a Full Professor and the Director of LIVIA, a research laboratory focused on computer vision and artificial intelligence. He is the FRQS Co-Chair in AI and Health, and the ÉTS Industrial Research Co-Chair on embedded neural networks for intelligent connected buildings (Distech Controls Inc.). His research interests include pattern recognition, machine learning, and computer vision, with applications in affective computing, biometrics, face recognition, medical image analysis, and video surveillance.